PLOS ONE

RESEARCH ARTICLE

Dissect the immunity using cytokine profiling and NF-kB target gene analysis in systemic inflammatory minipig model

Han Na Suh*☯, Young Kyu Kim☯, Ju Young Lee, Goo-Hwa Kang, Jeong Ho Hwang*

Animal Model Research Group, Korea Institute of Toxicology, Jeongeup, Jeollabuk-do, Republic of Korea

☯ These authors contributed equally to this work.
* hanna.suh@kitox.re.kr (HNS); jeongho.hwang@kitox.re.kr (JHH)

Abstract

Minipigs have remarkably similar physiology to humans, therefore, they it can be a good animal model for inflammation study. Thus, the conventional (serum chemistry, histopathology) and novel analytic tools [immune cell identification in tissue, cytokine level in peripheral blood mononuclear cells (PBMC) and serum, NF-kB target gene analysis in tissue] were applied to determine inflammation in Chicago Miniature Swine (CMS) minipig. Lipopolysaccharide (LPS)-induced acute systemic inflammation caused liver and kidney damage in serum chemistry and histopathology. Immunohistochemistry (IHC) also showed an increase of immune cell distribution in spleen and lung during inflammation. Moreover, NF-kB-target gene expression was upregulated in lung and kidney in acute inflammation and in heart, liver, and intestine in chronic inflammation. Cytokine mRNA was elevated in PBMC under acute inflammation along with elevated absolute cytokine levels in serum. Overall, LPS-mediated systemic inflammation affects the various organs, and can be detected by IHC of immune cells, gene analysis in PBMC, and measuring the absolute cytokine in serum along with conventional inflammation analytic tools.

Citation: Suh HN, Kim YK, Lee JY, Kang G-H, Hwang JH (2021) Dissect the immunity using cytokine profiling and NF-kB target gene analysis in systemic inflammatory minipig model. PLoS ONE 16(6): e0252947. https://doi.org/10.1371/journal.pone.0252947

Editor: Michal A. Olszewski, University of Michigan Health System, UNITED STATES

Received: January 14, 2021

Accepted: May 25, 2021

Published: June 4, 2021

Data Availability Statement: All relevant data are within the manuscript.

Funding: Korea Institute of Toxicology, KK-1911 & 2009-01, Mr Jeong Ho Hwang.

Competing interests: The authors have declared that no competing interests exist.

Introduction

Inflammation is a well-organized response of immune cells and biomolecules. When the body undergoes inflammation, it initiates eicosanoids, chemokines, and cytokines released by resident macrophages or mast cells, and then recruits neutrophils and lymphocytes. These combined responses induce typical inflammatory symptoms and pathophysiological conditions. Inflammation is classified as either acute or chronic based on duration or cause. Acute inflammation is rapid response initiated by infection or tissue damage which follows abnormal vascular permeability, blood flow, and nerve fiber sensitization [1]. Chronic inflammation is long-term response caused by repeated tissue injury and recovery [2] is closely linked with a number of diseases (ischemic disease, atherosclerosis, stroke, cancer, diabetes mellitus, non-alcoholic fatty liver disease) [3].

Inflammation animal models have been established to find new drugs and explore the pathophysiological mechanism of inflammation. To mimic a local inflammation (chemical-induced paw or ear edema animal model) [4] or systemic inflammation (LPS administration,

Escherichia coli inoculation, or cecal ligation and puncture), various methods are utilized [5]. Among them, LPS is a potent immune stimulator through CD14/toll-like receptor 4 (TLR4)/myeloid differentiation 2 (MD2) receptor in monocyte/macrophage. As LPS-induced cytokines mediate loss of function and immune cell infiltration in tissues, intravenous LPS provokes sepsis-like systemic inflammation [6]. Local LPS administration generates respiratory [7] or neural inflammation [8, 9]. LPS-challenged animal models show a rapid onset of inflammation and similar symptoms to humans. In addition, LPS affects both immune cells and parenchymal cells, including alveolar epithelial cells, myocardial cells, and kidney tubule cells [10–13], suggesting that LPS directly and indirectly modulates the immune response in various organs. Therefore, in this study, LPS was chosen to induce systemic inflammation in minipig model.

So far, rodents have been widely used as an inflammation animal model because cost effectiveness and easy of handling [14]. However, for LPS, a dose 10^6 times greater is required to induce similar symptoms in mice as in humans. Non-human primates (NHPs) are also used as inflammatory animal models due to their phylogenic proximity to humans. NHPs are more resistant to LPS than human [15, 16], but display an identical hemodynamic and cytokine response under LPS [15]. There is evidence that strong LPS resistance in mice is related with protein factors in rodent sera, which are absent in humans [17]. Immune system similarity may provide a better inflammatory animal model. Immune gene analysis revealed that porcine shows higher similarity, at DNA sequence level, to humans than mice [18]. In particular, porcine immune response shows 80% similarity as human than 10% similarity of mice [19]. Thus, the minipig was chosen as a systemic inflammatory animal model. In this study, the conventional diagnostic tools (serum chemistry, histopathology) are compared with direct immune cell detection (IHC) and LPS-induced gene expression in CMS minipig systemic inflammation model.

Materials and methods

Experimental animals

Six minipigs, (CMS, *Sus Scrofa*), 10 months-old, 19.60–24.65 kg body weight, were used. Two minipigs were randomly selected, based on body weight for each group. To establish the systemic inflammatory minipig model, 5 μg/kg LPS was administered seven times intramuscularly for chronic inflammation, and 25 μg/kg LPS was administered once intramuscularly for acute inflammation. Minipigs were housed under a 12 h/12 h light/dark cycle with lights on at 8 am. Water was provided *ad libitum* and food was provided at 2% of body weight per day. All the animal experiments were conducted under the Institutional Animal Care and Use Committee guideline of Korea Institute of Toxicology (IACUC approval # 19-1-0194, 20-1-0064).

Serum chemistry

For serum chemistry, blood was collected, incubated for 30 min at RT, and centrifuged for 10 min, 3,000 rpm at RT. Supernatant was isolated as serum. Serum chemistry was measured using TBA 120 FR chemistry analyzer (Toshiba Co., Japan).

Histological analysis

Histopathology. Tissues from target organs (kidney, liver) were fixed in 10% neutral buffered formalin (NBF) overnight and embedded in paraffin. Tissue samples were sectioned (5 μm), deparaffinized, and stained with hematoxylin and eosin (H&E) to determine structural abnormalities of kidney and liver. Glomeruli (black dot line) and proximal tubules were examined in kidney. Hepatic tissues near central vein (CV, black dot line) were examined in liver.

Immunohistochemistry. Tissues were fixed in 10% NBF overnight and embedded in paraffin. Tissue samples were then sectioned (5 μm), deparaffinized, processed for antigen retrieval, blocked, incubated with target primary antibody, and peroxidase-conjugated secondary antibody. Samples were mounted and photographed using microscopy (Leica DM2700). For peroxidase-conjugated secondary antibody, 3,3'-Diaminobenzidine (DAB) substrate was used, followed by hematoxylin for nuclear counterstaining.

Gene analysis

For gene expression analysis, tissues (heart, lung, kidney, liver, duodenum, PBMC) were processed for RNA extraction (QIAGEN RNeasy Mini Kit) and reverse transcription (iScript RT Supermix for RT-qPCR, Biorad). Glyceraldehyde-3-Phosphate Dehydrogenase (GAPDH) was used as an endogenous control for normalization. qRT-PCR was performed using intron-spanning primers. Fold induction was quantified using the $2^{-\Delta\Delta CT}$ method. In Fig 4A, values are displayed using Heatmap software (bar.utoronto.ca/). Primer sequences are listed on Table 1.

Enzyme-Linked Immunosorbent Assay (ELISA)

To measure the absolute cytokine level, serum was obtained at day 0 (pre-treatment), day 1~day7 (two hours after LPS administration], and day 8 (post-treatment). Porcine IL-1β (R&D, PLB00B), IL-6 (R&D, P6000B), TNFα (R&D, TPA00), IL-8 (Invitrogen, P8000), and IFNγ (R&D, DY985) were measured by the ELISA method according to the manufacturer's protocol. The absolute cytokine levels are shown in Table 2.

Statistical analyses

The student's *t*-test was used for comparisons of two samples. P values < 0.05 were considered significant. Error bars indicate standard deviation (SD). The number of biological replicates is 2 and experimental replicates is 3, unless otherwise mentioned in Figure Legends.

Table 1. Primers used for qRT-PCR.

Species	Gene symbol	Primer sequences (from 5' to 3')	Length	Gene Bank ID
Sus scrofa	*CRP*	F: AGGGCGCTGAGGTATGAAAT	117	NM_213844.2
		R: ACAAGGGGAACGTAAGGTGT		
	SOD1	F: AGGCCGTGTGTGTGCTGAA	117	NM_001190422.1
		R: GATCACCTTCAGCCAGTCCTTTA		
	IL-1β	F: GAGCATCAGGCAGATGGTGT	134	NM_214055.1
		R: CAAGGATGATGGGCTCTTCTTC		
	IL-6	F: GCTGCTTCTGGTGATGGCTACTGCC	318	NM_001252429.1
		R: TGAAACTCCACAAGACCGGTGGTGA		
	TNFα	F: ATGAGCACTGAGAGCATGATCCG	163	NM_214022.1
		R: CCTCGAAGTGCAGTAGGCAGA		
	COX2	F: TTCAACCAGCAATTCCAATACCA	87	NM_214321.1
		R: GAAGGCGTCAGGCAGAAG		
	TGFβ	F: AGGGCTACCATGCCAATTTCT	101	NM_214015.2
		R: CGGGTTGTGCTGGTTGTACA		
	IL-10	F: CGG CGC TGT CAT CAA TTT CTG	89	NM_214041.1
		R: CCC CTC TCT TGG AGC TTG CTA		
	GAPDH	F: ACAGACAGCCGTGTGTTCC	62	NM_001206359.1
		R: ACCTTCACCATCGTGTCTCA		

https://doi.org/10.1371/journal.pone.0252947.t001

Table 2. Absolute cytokine level after LPS induction.

	IL-1β (pg/ml)		IL-6 (pg/ml)		TNFα (pg/ml)	
	Chronic	**Acute**	**Chronic**	**Acute**	**Chronic**	**Acute**
D0	U.D.	U.D.	0.80 ± 0.51	5.02 ± 1.53	27.78 ± 1.50	88.21 ± 2.51
D1	39.03 ± 4.3	5.72 ± 1.16	977.5 ± 10.27	6.58 ± 0.37	2312 ± 49.54	74.74 ± 2.77
D2	135 ± 9.13	15.37 ± 8.61	80.89 ± 2.92	7.44 ± 0.60	749.9 ± 9.77	63.43 ± 2.15
D3	112.6 ± 10.73	5.036 ± 0.20	45.47 ± 1.42	5.1 ± 0.68	442.7 ± 4.09	75.46 ± 1.08
D4	40.57 ± 1.36	14.06 ± 6.85	12.43 ± 0.75	6.65 ± 1.27	210.6 ± 4.92	74.75 ± 1.24
D5	86.69 ± 10.52	11.38 ± 4.93	11.54 ± 2.66	6.26 ± 0.11	108.8 ± 3.89	81.88 ± 1.06
D6	23.69 ± 13.95	32.23± 16.89	7.06 ± 0.48	7.92 ± 1.17	114 ± 2.57	77.19 ± 2.15
D7	63.62 ± 7.58	716.3 ± 6.21	15.99 ± 1.09	2218 ± 122.3	111.4 ± 0.95	9224 ± 1218
D8	21.37 ± 6.14	96.22 ± 5.23	2.35 ± 0.46	30.05 ± 0.64	25.72 ± 1.65	1992 ± 48.81
	IL-8 (pg/ml)		**IFNγ (pg/ml)**			
	Chronic	**Acute**	**Chronic**	**Acute**		
D0	72.08 ± 0.98	47.54 ± 2.53	U.D.	U.D.		
D1	855.4 ± 50.91	39.32 ± 2.08	U.D.	U.D.		
D2	673.7 ± 15.56	18.21 ± 1.16	U.D.	U.D.		
D3	196.3 ± 3.16	87.64 ± 1.61	U.D.	U.D.		
D4	36.74 ± 1.72	29.62 ± 1.58	U.D.	U.D.		
D5	35.23 ± 1.13	18.39 ± 1.47	U.D.	U.D.		
D6	40.64 ± 1.56	55.81 ± 1.54	U.D.	U.D.		
D7	20.19 ± 1.41	2361 ± 140.8	U.D.	39.79 ± 4.55		
D8	23.64 ± 0.37	2.48 ± 2.60	U.D.	U.D.		

https://doi.org/10.1371/journal.pone.0252947.t002

Results

Determination of LPS-induced systemic inflammation

To develop the systemic inflammatory minipig model, seven doses of 5 μg/kg LPS were administrated for chronic inflammation, and one dose of 25 μg/kg LPS was administrated for acute inflammation (Fig 1A). To determine whether LPS induces organ damage, analyses of serum chemistry and histopathology were performed. LPS increased blood urea nitrogen (BUN) and aspartate aminotransferase (AST) in acute inflammation at day 8 (Fig 1B), indicating kidney and liver damage. H&E staining showed lymphoid infiltration in renal cortical interstitial, without glomeruli abnormality, and hydropic change of hepatocytes in acute inflammation (black arrowhead) (Fig 1C). There were no changes in serum chemistry and histopathology in chronic inflammation. These results show that LPS-induced systemic acute inflammation injures the kidney and liver, which is diagnosed by serum chemistry and histopathology.

The spleen filters and stores blood, therefore, the population of circulating immune cells can be measured in this organ. Thus, the IHC of immune cells following LPS induction was determined. The number of CD11b+, MPO+, CD4+, and CD8+ cells was slightly increased in chronic inflammation, whereas it massively increased in acute inflammation (Fig 2A–2D). These results indicate that IHC accurately detects the type and distribution of various immune cells. LPS induction establishes successful systemic inflammatory minipig model, and the direct detection of immune cells and serum chemistry compensate for inflammation diagnosis.

Immune cell dynamics in LPS-induced pulmonary inflammation

As the respiratory tract is directly connected with the outside of the body, alveolar macrophage is activated to remove foreign bodies in lung [20]. The function of other immune cells during

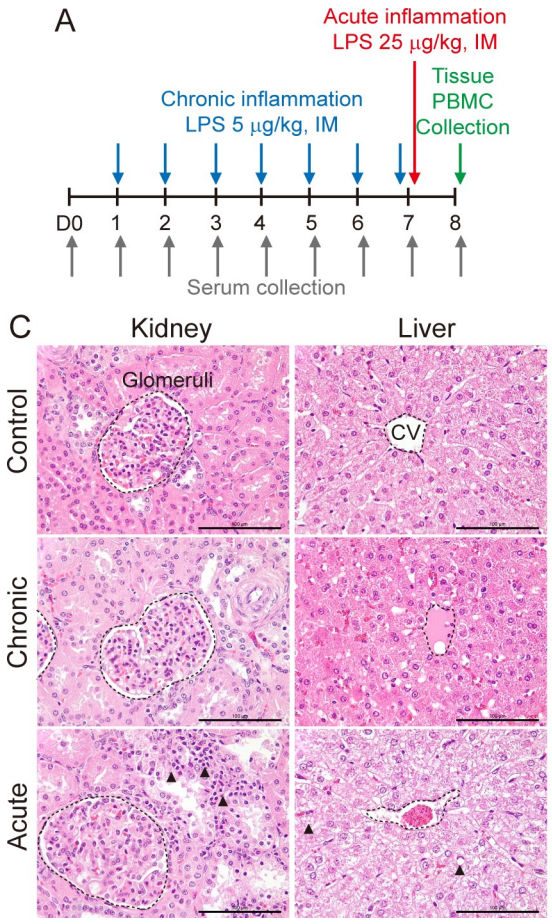

B

	Control	Chronic	Acute
GLU (mg/dL)	87.15 ± 9.75	80.35 ± 2.05	84.1 ± 18.9
BUN (mg/dL)	9.6 ± 0.7	9.7 ± 1.5	30.75 ± 1.95 #
CREA (mg/dL)	1.14 ± 0.03	1.2 ± 0.05	1.46 ± 0.13
AST (IU/L)	36.95 ± 15.05	43.3 ± 24.9	63.65 ± 19.75
ALT (IU/L)	28.4 ± 1	25.8 ± 1.5	26.7 ± 1.4

#P < 0.05

Fig 1. Comparison of serum chemistry and histopathology. (A) Experimental schematic: For chronic inflammation, 5 μg/kg lipopolysaccharide (LPS) was administrated, intramuscularly (IM), seven times, daily. For acute inflammation, 25 μg/kg LPS was administrated, IM, once at day7. Two CMS minipigs were used for each group (control, chronic, acute). Blood and tissue were sampled for further study. **(B)** Serum chemistry was measured using a TBA 120 FR chemistry analyzer (Toshiba Co., Japan). Absolute values are indicated. #$P<0.05$. **(C)** H&E staining. Glomeruli in kidney and central vein in liver are indicated with a black dot line. Abnormal lesions are indicated with black arrow head. Scale bar = 100 μm.

https://doi.org/10.1371/journal.pone.0252947.g001

homeostasis or inflammation are less well known. Thus, macrophages, neutrophils, and lymphocytes in the lung were detected after LPS induction using IHC. CD11b+ and MPO+ cells were identified, while CD4+ and CD8+ cells were not found in normal lung. All four types of immune cell were elevated in the alveoli during acute inflammation (Fig 3A–3D). Especially, CD4+ and CD8+ T lymphocytes significantly infiltrated alveoli after LPS induction. These results suggest that systemic inflammation regulates immune cell dynamics and infiltration into the damaged lung.

Inflammation-related gene expression in tissue and PBMC

TLR4 has been identified in parenchymal organs including heart [21], lung [22], liver [23], kidney [24], and intestine [25], which suggests that LPS might directly affect these organs. LPS-bound TLR4 upregulates transcription factor NF-kB and numerous target gene synthesis, subsequently. Thus, to determine the effect of LPS on NF-kB target gene expression [26–29], the expression of cytokine (*IL-6*), acute phase inflammation response (*CRP*), pro-inflammatory (*COX-2*), and anti-oxidant (*SOD1*) was measured. Chronic cardiac inflammation

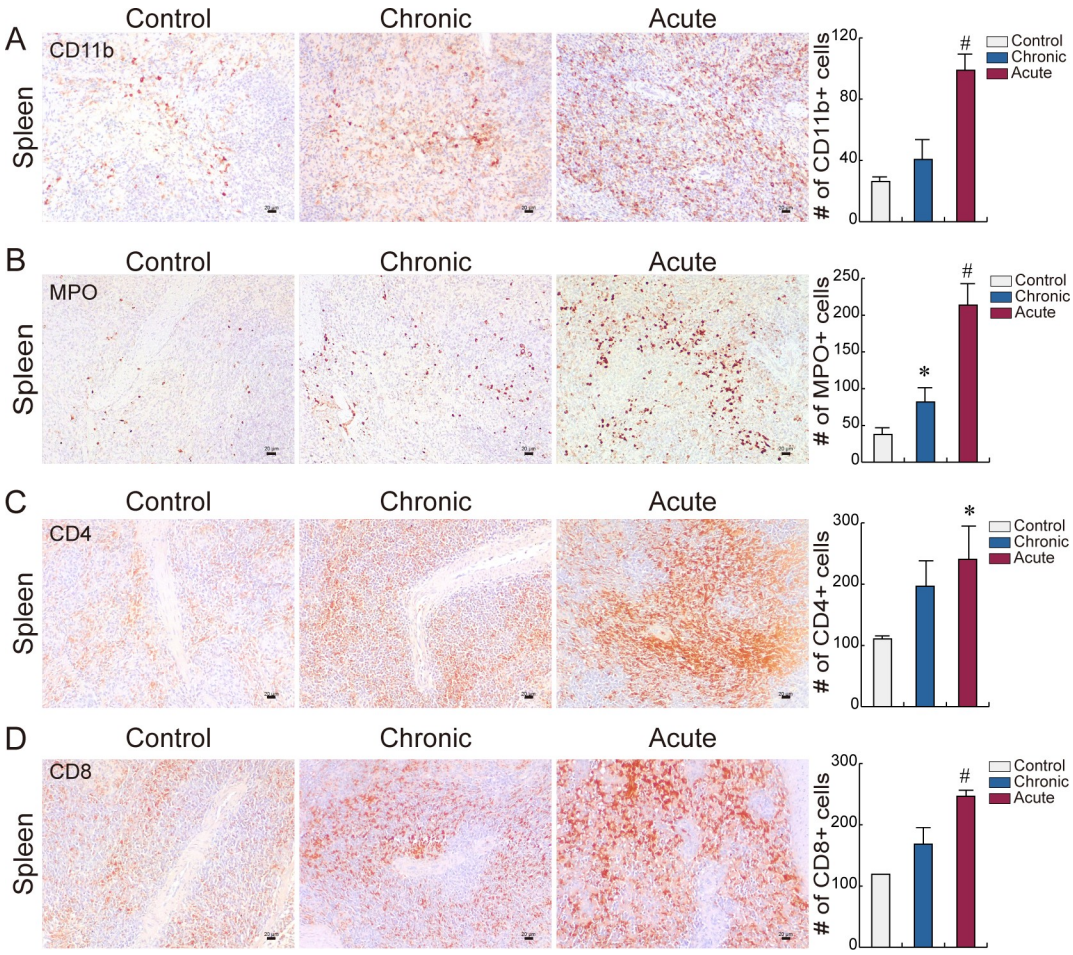

Fig 2. Immune cell distribution in spleen. (A–D) Immunohistochemistry. Population and distribution of **(A)** CD11b+ (macrophage), **(B)** MPO+ (neutrophil), **(C)** CD4+, and **(D)** CD8+ (lymphocyte) cells were examined in spleen. Representative images are shown; N≥3. Quantification of the immune cell number is shown as mean ± SD; $^{\#}P<0.01$ relative to control, $^{*}P<0.05$ relative to control. Scale bar = 20 μm.

https://doi.org/10.1371/journal.pone.0252947.g002

upregulated *CRP* (1.1 fold change), *COX-2* (1.37), and *SOD1* (0.69), while acute upregulated *IL-6* (0.52). Chronic pulmonary inflammation decreased the *COX-2* (-1.61) and *SOD1* (-2.26) mRNA expression, while acute increased *IL-6* (3.29), *CRP* (12.64), *COX-2* (4.00), and *SOD1* (5.39) mRNA expression. Only *CRP* (5.62) was upregulated during chronic hepatic inflammation. The expression of *COX-2* (2.11) was increased in acute inflammation of kidney. In the intestine, LPS upregulated all four genes during chronic inflammation [*IL-6* (1.64), *CRP* (0.57), *COX-2* (4.30), and *SOD1* (1.06); Fig 4A]. These data suggest that each organ has different sensitivity to LPS (lung and kidney: immediate response; heart, liver, duodenum: delayed response) and each organ shows specific target gene upregulation.

To determine the synthesis of biomolecules in immune cells, PBMC was isolated and cytokine mRNA expression was analyzed. In chronic inflammation, both pro-inflammatory and anti-inflammatory genes were suppressed. In acute inflammation, pro-inflammatory genes (*IL-1β*, *IL-6*, *TNFα*, *COX-2*) were upregulated, while anti-inflammatory genes (*TGFβ*, *IL-10*) were downregulated (Fig 4B). PBMC which is stimulated by multiple low dose LPS downregulated the cytokine synthesis, suggesting attenuation of the immune response. In addition,

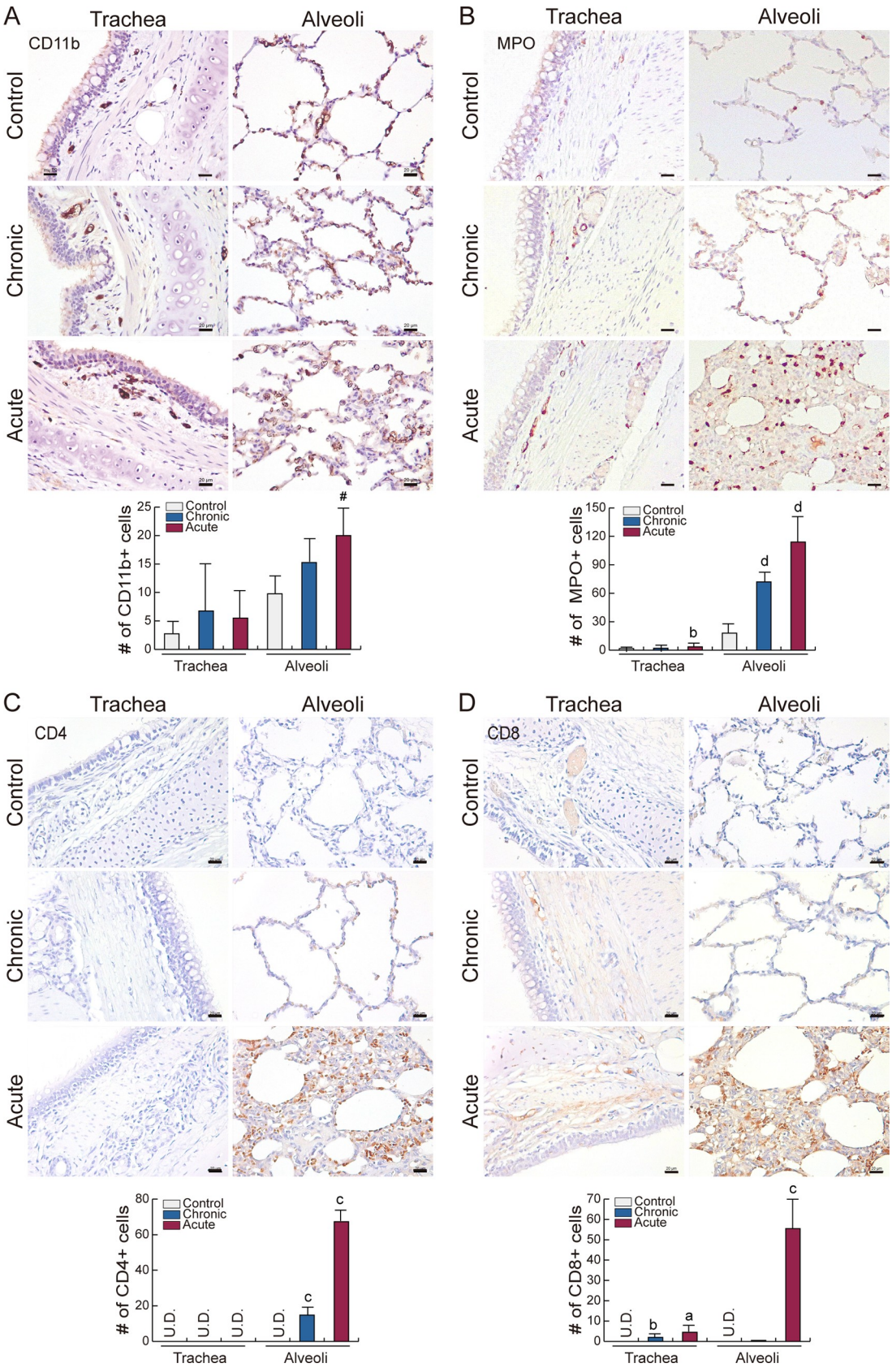
A
Trachea
Alveoli
CD11b
Control
Chronic
Acute
# of CD11b+ cells
Control
Chronic
Acute
#
Trachea
Alveoli
B
Trachea
Alveoli
MPO
Control
Chronic
Acute
# of MPO+ cells
Control
Chronic
Acute
b
d
d
Trachea
Alveoli
C
Trachea
Alveoli
CD4
Control
Chronic
Acute
# of CD4+ cells
Control
Chronic
Acute
U.D.
U.D.
U.D.
U.D.
c
c
Trachea
Alveoli
D
Trachea
Alveoli
CD8
Control
Chronic
Acute
# of CD8+ cells
Control
Chronic
Acute
U.D.
b
a
U.D.
c
Trachea
Alveoli

Fig 3. Immune cell distribution in lung. (A–D) Immunohistochemistry. Population and distribution of **(A)** CD11b+ (macrophage), **(B)** MPO+ (neutrophil), **(C)** CD4+, and **(D)** CD8+ (lymphocyte) cells were examined in lung. Representative images are shown; N≥3. Quantification of the immune cell number is shown as mean ± SD; [a]$P<0.01$ relative to trachea control, [b]$P<0.05$ relative to trachea control, [c]$P<0.01$ relative to alveoli control, [d]$P<0.05$ relative to alveoli control. Scale bar = 20 μm.

https://doi.org/10.1371/journal.pone.0252947.g003

single high dose LPS enhanced the pro-inflammatory cytokine synthesis, suggesting activation of the immune response.

Absolute cytokine level after LPS-induced systemic inflammation

To determine the inflammatory cytokine response after LPS induction, cytokines were detected in serum at various time points using ELISA. In chronic inflammation, the peak concentration of IL-6, TNFα, and IL-8 was two hours after the first LPS administration (5 μg/kg) and then cytokine levels gradually decreased despite daily LPS administration (Fig 5B–5D, Table 2). Moreover, IL-1β expression showed a delay in peak concentration after the second LPS challenge, and cytokine level was fluctuated until day 8 (Fig 5A, Table 2). IFNγ was not

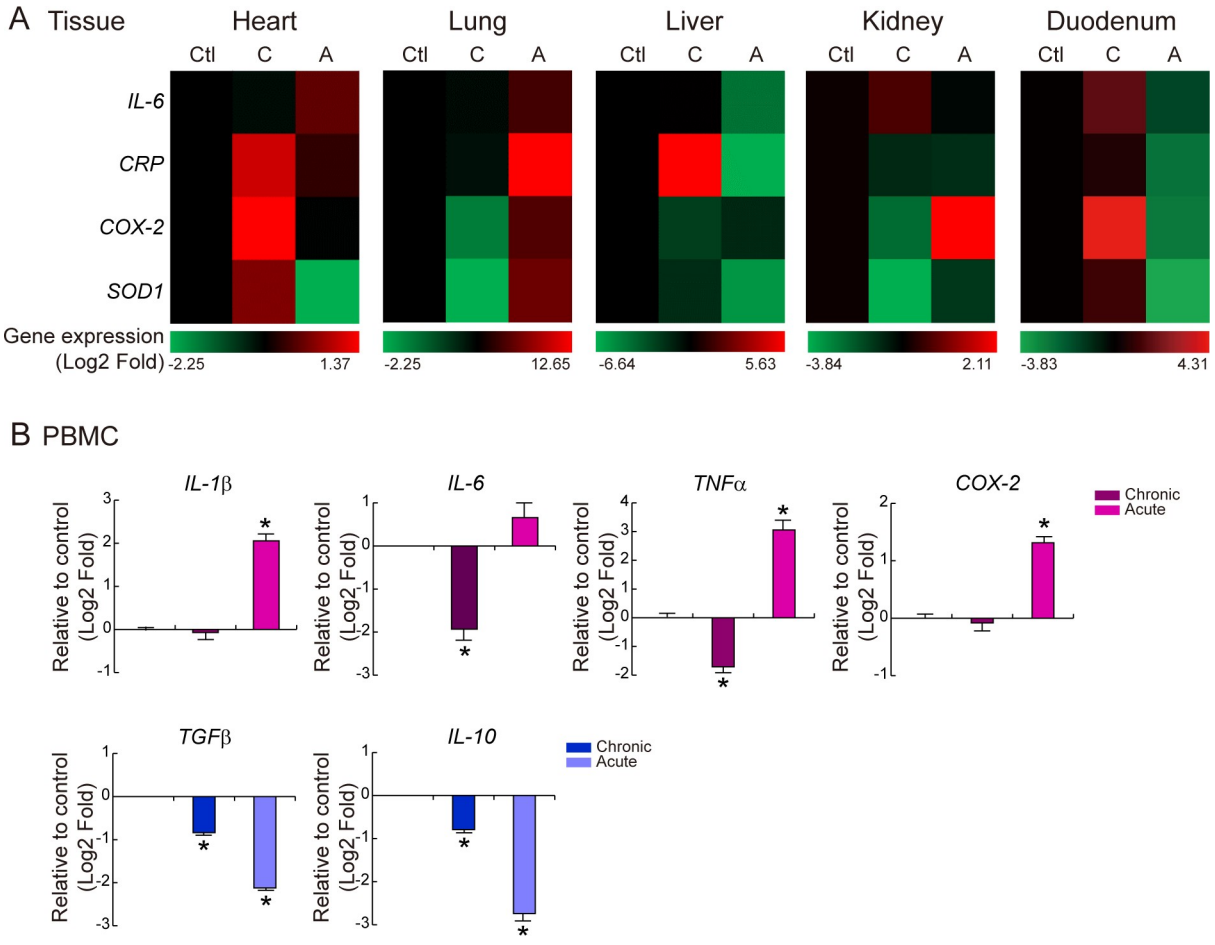

Fig 4. Inflammation-related gene expression in tissues and PBMC. (A) qRT-PCR and Heatmap in tissues. *IL-6*, *CRP*, *COX-2*, *SOD1* mRNA expression were analyzed in heart, lung, liver, kidney, and duodenum under chronic and acute inflammation with two biological and three experimental replicates. Red color indicates gene upregulation and green color indicates gene downregulation. **(B)** qRT-PCR in PBMC. Pro-inflammatory (*IL-1β*, *IL-6*, *TNFα*, *COX-2*) and anti-inflammatory (*TGFβ*, *IL-10*) mRNA expression were analyzed in PBMC under chronic and acute inflammation with two biological and three experimental replicates.

https://doi.org/10.1371/journal.pone.0252947.g004

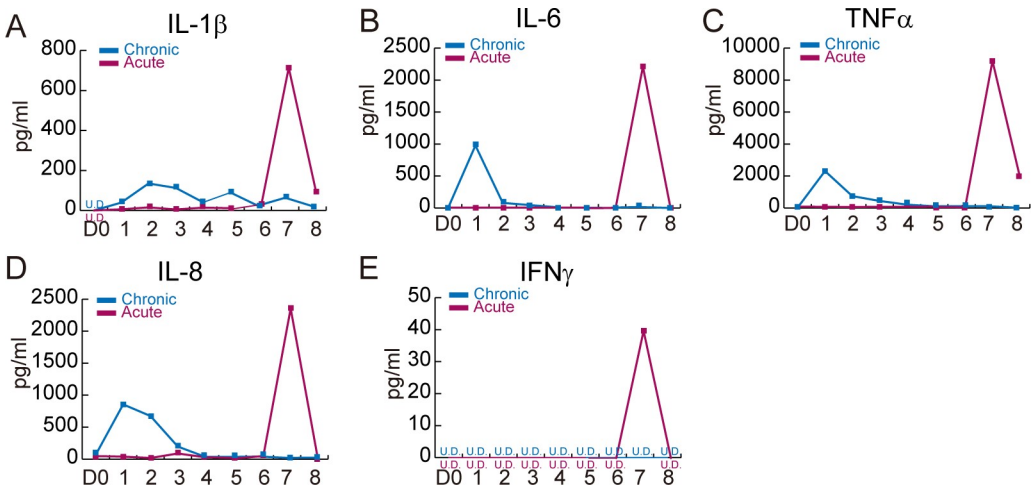

Fig 5. Serum cytokine analysis using ELISA. Blood was collected at day 0, 1, 2, 3, 4, 5, 6, 7, and 8 and then serum was isolated. Absolute cytokine levels (pg/ml) were measured by ELISA with two biological and three experimental replicates. **(A)** IL-1β, **(B)** IL-6, **(C)** TNFα, **(D)** IL-8, **(E)** IFNγ. U.D. = undetected.

https://doi.org/10.1371/journal.pone.0252947.g005

detected (Fig 5E, Table 2). In acute inflammation, all five cytokines reached their peak level two hours after LPS administration (25 μg/kg) (Fig 5A–5E, Table 2). The basal level of cytokines showed the variation in homeostasis (Fig 5, IL-1β: undetected, IL-6: 0.797 pg/ml, TNFα: 27.78 pg/ml, IL-8: 72.08 pg/ml, IFNγ: undetected). All five cytokines were upregulated by LPS both chronic and acute. However, the elevated level of cytokine was much higher in acute LPS induction compared to day 0. Interestingly, the cytokine level at day 8 returned to similar level as day 0.

Discussion

In this study, inflammation-related gene expression in organs (heart, lung, liver, kidney, intestine), cytokine mRNA in PBMC, absolute cytokine in serum, and immune cell population in tissue were analyzed after LPS induction in CMS minipig. Rodent models are attractive inflammatory model due to cost effectiveness but their body size limits hemodynamic monitoring [14, 30, 31]. LPS modulation on the immune response is well characterized in NHP because of the close phylogenic relationship [32, 33]. In this study, the CMS minipig was used as a systemic inflammatory animal model. Porcine have different pulmonary vascular physiology to humans in systemic inflammation [31]. However, its high similarity in immune genes suggest that porcine can be another representative inflammatory animal model. The immune response is an effective process involving immune cells and cytokines. Acute inflammation increased the number of immune cells and distribution of all four immune cells (CD11b+ macrophage, MPO+ neutrophil, CD4+ lymphocyte, CD8+ lymphocyte) (Fig 2A–2D). Also, mRNA levels of pro-inflammatory cytokines in PBMC was upregulated (Fig 4B). Furthermore, cytokine level in serum was elevated after LPS induction (Fig 5). These results shows that LPS regulates the immune response, including immune cell dynamics, cytokine synthesis in immune cells, and elevation of cytokine in serum. 5 μg/kg LPS, seven times, IM administration induces mild and prolonged immune response indicating slight increase of immune cell population and serum cytokine level. Also, 25 μg/kg LPS, once, IM administration induces strong immune cell response indicating massive increase of immune cell population and serum cytokine level. Thus, in this study, a stable and affordable inflammatory minipig model and analytic tools for inflammation has been established.

Bacterial LPS mediates the sepsis and immune response, which leads to tissue damage and organ failure [34]. Especially, LPS-treated liver and kidney failure have been reported, which were diagnosed by serum chemistry [35, 36]. As AST is located in the cytosol and mitochondria of hepatocytes, and alanine aminotransferase (ALT) is situated in the cytosol of hepatocyte, elevation of AST or ALT in serum is the most relevant marker of hepatic injury. BUN and creatinine levels are also elevated when renal clearance fails. In this study, we have found that LPS-induced BUN and AST elevation (Fig 1B) and *COX-2* upregulation in acute renal inflammation and *CRP* upregulation in chronic hepatic inflammation (Fig 4A). Previous studies support our findings. Enhanced COX-2 is considered a renal pathological condition as COX-2 regulates tubular reabsorption and glomeruli filtration [37–39]. As CRP is synthesized in hepatocytes, elevated CRP is related to hepatic damage [40]. These results show that LPS mediates organ damage and organ-specific gene upregulation under inflammation. Thus, organ-specific target genes can be analytic tools for inflammation.

Pulmonary inflammation was significantly affected by acute inflammation, as demonstrated by immune cell infiltration and NF-kB target gene (*IL-6*, *CRP*, *COX-2*, *SOD1*) upregulation (Figs 3 and 4A). Moreover, those genes were downregulated in chronic inflammation even though there was a slight increase of immune cell infiltration. This could be because activated neutrophil or macrophage regenerate the lung and attenuate the inflammation [41, 42]. Of note, NF-kB target genes were upregulated in heart and intestine during chronic inflammation (Fig 4A) which indicates that these organs are affected by the long-term immune response [43, 44]. These findings suggest that each organ has distinct LPS sensitivity (acute or chronic), and LPS-induced tissue damage has various mechanisms (specific target). It is noteworthy examining a serum chemistry and a histopathology to determine the organ damage. However, it does not completely reflect the various disease conditions, such as organ specific damage and injury/recovery status. In this study, we have developed LPS-induced systemic acute or chronic inflammation minipig model proven by immune cell population, cytokine mRNA expression in PBMC, and cytokine level in serum. Also, we have found that organ specific gene activation with various mechanism under systemic inflammation.

Conclusions

LPS-mediated systemic inflammation affects the organs and novel analytic tools such as IHC of immune cells, cytokine mRNA analysis in PBMC, and absolute cytokine analysis in serum support conventional inflammation detection tools.

Author Contributions

Formal analysis: Han Na Suh.

Funding acquisition: Jeong Ho Hwang.

Methodology: Han Na Suh, Young Kyu Kim, Ju Young Lee, Goo-Hwa Kang.

Software: Young Kyu Kim.

Supervision: Jeong Ho Hwang.

Visualization: Han Na Suh.

Writing – original draft: Han Na Suh.

Writing – review & editing: Han Na Suh.

References

1. Kulkarni RG, Achaiah G, Sastry GN. Novel targets for antiinflammatory and antiarthritic agents. Curr Pharm Des. 2006; 12(19):2437–54. Epub 2006/07/18. https://doi.org/10.2174/138161206777698945 PMID: 16842190.
2. Chung HJ, Lee HS, Shin JS, Lee SH, Park BM, Youn YS, et al. Modulation of acute and chronic inflammatory processes by a traditional medicine preparation GCSB-5 both in vitro and in vivo animal models. J Ethnopharmacol. 2010; 130(3):450–9. Epub 2010/07/14. https://doi.org/10.1016/j.jep.2010.05.020 PMID: 20621661.
3. Andreasen AS, Krabbe KS, Krogh-Madsen R, Taudorf S, Pedersen BK, Moller K. Human endotoxemia as a model of systemic inflammation. Curr Med Chem. 2008; 15(17):1697–705. Epub 2008/08/05. https://doi.org/10.2174/092986708784872393 PMID: 18673219.
4. Patil KR, Mahajan UB, Unger BS, Goyal SN, Belemkar S, Surana SJ, et al. Animal Models of Inflammation for Screening of Anti-inflammatory Drugs: Implications for the Discovery and Development of Phytopharmaceuticals. Int J Mol Sci. 2019; 20(18). Epub 2019/09/08. https://doi.org/10.3390/ijms20184367 PMID: 31491986; PubMed Central PMCID: PMC6770891.
5. Stortz JA, Raymond SL, Mira JC, Moldawer LL, Mohr AM, Efron PA. Murine Models of Sepsis and Trauma: Can We Bridge the Gap? ILAR J. 2017; 58(1):90–105. Epub 2017/04/27. https://doi.org/10.1093/ilar/ilx007 PMID: 28444204; PubMed Central PMCID: PMC5886315.
6. Chen L, Welty-Wolf KE, Kraft BD. Nonhuman primate species as models of human bacterial sepsis. Lab Anim (NY). 2019; 48(2):57–65. Epub 2019/01/16. https://doi.org/10.1038/s41684-018-0217-2 PMID: 30643274; PubMed Central PMCID: PMC6613635.
7. Seehase S, Lauenstein HD, Schlumbohm C, Switalla S, Neuhaus V, Forster C, et al. LPS-induced lung inflammation in marmoset monkeys—an acute model for anti-inflammatory drug testing. PLoS One. 2012; 7(8):e43709. Epub 2012/09/07. https://doi.org/10.1371/journal.pone.0043709 PMID: 22952743; PubMed Central PMCID: PMC3429492.
8. Zhao J, Bi W, Xiao S, Lan X, Cheng X, Zhang J, et al. Neuroinflammation induced by lipopolysaccharide causes cognitive impairment in mice. Sci Rep. 2019; 9(1):5790. Epub 2019/04/10. https://doi.org/10.1038/s41598-019-42286-8 PMID: 30962497; PubMed Central PMCID: PMC6453933.
9. Sheppard O, Coleman MP, Durrant CS. Lipopolysaccharide-induced neuroinflammation induces presynaptic disruption through a direct action on brain tissue involving microglia-derived interleukin 1 beta. J Neuroinflammation. 2019; 16(1):106. Epub 2019/05/20. https://doi.org/10.1186/s12974-019-1490-8 PMID: 31103036; PubMed Central PMCID: PMC6525970.
10. Liu L, Wang Y, Cao ZY, Wang MM, Liu XM, Gao T, et al. Up-regulated TLR4 in cardiomyocytes exacerbates heart failure after long-term myocardial infarction. J Cell Mol Med. 2015; 19(12):2728–40. Epub 2015/08/21. https://doi.org/10.1111/jcmm.12659 PMID: 26290459; PubMed Central PMCID: PMC4687701.
11. de Laat MA, Gruntmeir KJ, Pollitt CC, McGowan CM, Sillence MN, Lacombe VA. Hyperinsulinemia Down-Regulates TLR4 Expression in the Mammalian Heart. Front Endocrinol (Lausanne). 2014; 5:120. Epub 2014/08/08. https://doi.org/10.3389/fendo.2014.00120 PMID: 25101057; PubMed Central PMCID: PMC4105691.
12. Pulskens WP, Rampanelli E, Teske GJ, Butter LM, Claessen N, Luirink IK, et al. TLR4 promotes fibrosis but attenuates tubular damage in progressive renal injury. J Am Soc Nephrol. 2010; 21(8):1299–308. Epub 2010/07/03. https://doi.org/10.1681/ASN.2009070722 PMID: 20595685; PubMed Central PMCID: PMC2938595.
13. Xu D, Yan S, Wang H, Gu B, Sun K, Yang X, et al. IL-29 Enhances LPS/TLR4-Mediated Inflammation in Rheumatoid Arthritis. Cell Physiol Biochem. 2015; 37(1):27–34. Epub 2015/08/19. https://doi.org/10.1159/000430330 PMID: 26278073.
14. Fink MP. Animal models of sepsis. Virulence. 2014; 5(1):143–53. Epub 2013/09/12. https://doi.org/10.4161/viru.26083 PMID: 24022070; PubMed Central PMCID: PMC3916368.
15. Haudek SB, Natmessnig BE, Furst W, Bahrami S, Schlag G, Redl H. Lipopolysaccharide dose response in baboons. Shock. 2003; 20(5):431–6. Epub 2003/10/16. https://doi.org/10.1097/01.shk.0000090843.66556.74 PMID: 14560107.
16. Fiedler VB, Loof I, Sander E, Voehringer V, Galanos C, Fournel MA. Monoclonal antibody to tumor necrosis factor—alpha prevents lethal endotoxin sepsis in adult rhesus monkeys. J Lab Clin Med. 1992; 120(4):574–88. Epub 1992/10/01. PMID: 1402333.
17. Warren HS, Fitting C, Hoff E, Adib-Conquy M, Beasley-Topliffe L, Tesini B, et al. Resilience to bacterial infection: difference between species could be due to proteins in serum. J Infect Dis. 2010; 201(2):223–32. Epub 2009/12/17. https://doi.org/10.1086/649557 PMID: 20001600; PubMed Central PMCID: PMC2798011.

18. Wernersson R, Schierup MH, Jorgensen FG, Gorodkin J, Panitz F, Staerfeldt HH, et al. Pigs in sequence space: a 0.66X coverage pig genome survey based on shotgun sequencing. BMC Genomics. 2005; 6:70. Epub 2005/05/12. https://doi.org/10.1186/1471-2164-6-70 PMID: 15885146; PubMed Central PMCID: PMC1142312.

19. Dawson HD, Loveland JE, Pascal G, Gilbert JG, Uenishi H, Mann KM, et al. Structural and functional annotation of the porcine immunome. BMC Genomics. 2013; 14:332. Epub 2013/05/17. https://doi.org/10.1186/1471-2164-14-332 PMID: 23676093; PubMed Central PMCID: PMC3658956.

20. Iwasaki A, Foxman EF, Molony RD. Early local immune defences in the respiratory tract. Nat Rev Immunol. 2017; 17(1):7–20. Epub 2016/11/29. https://doi.org/10.1038/nri.2016.117 PMID: 27890913; PubMed Central PMCID: PMC5480291.

21. Yang Y, Lv J, Jiang S, Ma Z, Wang D, Hu W, et al. The emerging role of Toll-like receptor 4 in myocardial inflammation. Cell Death Dis. 2016; 7:e2234. Epub 2016/05/27. https://doi.org/10.1038/cddis.2016.140 PMID: 27228349; PubMed Central PMCID: PMC4917669.

22. Jia H, Sodhi CP, Yamaguchi Y, Lu P, Martin LY, Good M, et al. Pulmonary Epithelial TLR4 Activation Leads to Lung Injury in Neonatal Necrotizing Enterocolitis. J Immunol. 2016; 197(3):859–71. Epub 2016/06/17. https://doi.org/10.4049/jimmunol.1600618 PMID: 27307558; PubMed Central PMCID: PMC4955761.

23. Guo J, Friedman SL. Toll-like receptor 4 signaling in liver injury and hepatic fibrogenesis. Fibrogenesis Tissue Repair. 2010; 3:21. Epub 2010/10/23. https://doi.org/10.1186/1755-1536-3-21 PMID: 20964825; PubMed Central PMCID: PMC2984459.

24. Wu H, Chen G, Wyburn KR, Yin J, Bertolino P, Eris JM, et al. TLR4 activation mediates kidney ischemia/reperfusion injury. J Clin Invest. 2007; 117(10):2847–59. Epub 2007/09/15. https://doi.org/10.1172/JCI31008 PMID: 17853945; PubMed Central PMCID: PMC1974864.

25. Price AE, Shamardani K, Lugo KA, Deguine J, Roberts AW, Lee BL, et al. A Map of Toll-like Receptor Expression in the Intestinal Epithelium Reveals Distinct Spatial, Cell Type-Specific, and Temporal Patterns. Immunity. 2018; 49(3):560–75 e6. Epub 2018/09/02. https://doi.org/10.1016/j.immuni.2018.07.016 PMID: 30170812; PubMed Central PMCID: PMC6152941.

26. Ackerman WEt Summerfield TL, Vandre DD Robinson JM, Kniss DA. Nuclear factor-kappa B regulates inducible prostaglandin E synthase expression in human amnion mesenchymal cells. Biol Reprod. 2008; 78(1):68–76. Epub 2007/10/12. https://doi.org/10.1095/biolreprod.107.061663 PMID: 17928629.

27. Agrawal A, Samols D, Kushner I. Transcription factor c-Rel enhances C-reactive protein expression by facilitating the binding of C/EBPbeta to the promoter. Mol Immunol. 2003; 40(6):373–80. Epub 2003/10/03. https://doi.org/10.1016/s0161-5890(03)00148-2 PMID: 14522018.

28. Das KC, Lewis-Molock Y, White CW. Activation of NF-kappa B and elevation of MnSOD gene expression by thiol reducing agents in lung adenocarcinoma (A549) cells. Am J Physiol. 1995; 269(5 Pt 1):L588–602. Epub 1995/11/01. https://doi.org/10.1152/ajplung.1995.269.5.L588 PMID: 7491977.

29. Son YH, Jeong YT, Lee KA, Choi KH, Kim SM, Rhim BY, et al. Roles of MAPK and NF-kappaB in interleukin-6 induction by lipopolysaccharide in vascular smooth muscle cells. J Cardiovasc Pharmacol. 2008; 51(1):71–7. Epub 2008/01/23. https://doi.org/10.1097/FJC.0b013e31815bd23d PMID: 18209571.

30. Buras JA, Holzmann B, Sitkovsky M. Animal models of sepsis: setting the stage. Nat Rev Drug Discov. 2005; 4(10):854–65. Epub 2005/10/15. https://doi.org/10.1038/nrd1854 PMID: 16224456.

31. Zanotti-Cavazzoni SL, Goldfarb RD. Animal models of sepsis. Crit Care Clin. 2009; 25(4):703–19, vii-viii. Epub 2009/11/07. https://doi.org/10.1016/j.ccc.2009.08.005 PMID: 19892248.

32. Leturcq DJ, Moriarty AM, Talbott G, Winn RK, Martin TR, Ulevitch RJ. Antibodies against CD14 protect primates from endotoxin-induced shock. J Clin Invest. 1996; 98(7):1533–8. Epub 1996/10/01. https://doi.org/10.1172/JCI118945 PMID: 8833900; PubMed Central PMCID: PMC507584.

33. Wagner TL, Horton VL, Carlson GL, Myhre PE, Gibson SJ, Imbertson LM, et al. Induction of cytokines in cynomolgus monkeys by the immune response modifiers, imiquimod, S-27609 and S-28463. Cytokine. 1997; 9(11):837–45. Epub 1998/02/07. https://doi.org/10.1006/cyto.1997.0239 PMID: 9367544.

34. Cohen J. The immunopathogenesis of sepsis. Nature. 2002; 420(6917):885–91. Epub 2002/12/20. https://doi.org/10.1038/nature01326 PMID: 12490963.

35. Liaudet L, Murthy KG, Mabley JG, Pacher P, Soriano FG, Salzman AL, et al. Comparison of inflammation, organ damage, and oxidant stress induced by Salmonella enterica serovar Muenchen flagellin and serovar Enteritidis lipopolysaccharide. Infect Immun. 2002; 70(1):192–8. Epub 2001/12/19. https://doi.org/10.1128/IAI.70.1.192-198.2002 PMID: 11748182; PubMed Central PMCID: PMC127621.

36. Plotnikov EY, Brezgunova AA, Pevzner IB, Zorova LD, Manskikh VN, Popkov VA, et al. Mechanisms of LPS-Induced Acute Kidney Injury in Neonatal and Adult Rats. Antioxidants (Basel). 2018; 7(8). Epub 2018/08/12. https://doi.org/10.3390/antiox7080105 PMID: 30096767; PubMed Central PMCID: PMC6115895.

37. Ahmetaj-Shala B, Kirkby NS, Knowles R, Al'Yamani M, Mazi S, Wang Z, et al. Evidence that links loss of cyclooxygenase-2 with increased asymmetric dimethylarginine: novel explanation of cardiovascular side effects associated with anti-inflammatory drugs. Circulation. 2015; 131(7):633–42. Epub 2014/12/11. https://doi.org/10.1161/CIRCULATIONAHA.114.011591 PMID: 25492024; PubMed Central PMCID: PMC4768634.

38. Norregaard R, Kwon TH, Frokiaer J. Physiology and pathophysiology of cyclooxygenase-2 and prostaglandin E2 in the kidney. Kidney Res Clin Pract. 2015; 34(4):194–200. Epub 2016/01/19. https://doi.org/10.1016/j.krcp.2015.10.004 PMID: 26779421; PubMed Central PMCID: PMC4688592.

39. DeMaria AN, Weir MR. Coxibs—beyond the GI tract: renal and cardiovascular issues. J Pain Symptom Manage. 2003; 25(2 Suppl):S41–9. Epub 2003/02/27. https://doi.org/10.1016/s0885-3924(02)00630-9 PMID: 12604156.

40. Hurlimann J, Thorbecke GJ, Hochwald GM. The liver as the site of C-reactive protein formation. J Exp Med. 1966; 123(2):365–78. Epub 1966/02/01. https://doi.org/10.1084/jem.123.2.365 PMID: 4379352; PubMed Central PMCID: PMC2138142.

41. Hyde DM, Miller LA, McDonald RJ, Stovall MY, Wong V, Pinkerton KE, et al. Neutrophils enhance clearance of necrotic epithelial cells in ozone-induced lung injury in rhesus monkeys. Am J Physiol. 1999; 277(6):L1190–8. Epub 1999/12/22. https://doi.org/10.1152/ajplung.1999.277.6.L1190 PMID: 10600890.

42. Johnston LK, Rims CR, Gill SE, McGuire JK, Manicone AM. Pulmonary macrophage subpopulations in the induction and resolution of acute lung injury. Am J Respir Cell Mol Biol. 2012; 47(4):417–26. Epub 2012/06/23. https://doi.org/10.1165/rcmb.2012-0090OC PMID: 22721830; PubMed Central PMCID: PMC3927911.

43. Rose NR. Myocarditis: infection versus autoimmunity. J Clin Immunol. 2009; 29(6):730–7. Epub 2009/10/15. https://doi.org/10.1007/s10875-009-9339-z PMID: 19826933.

44. Barker N, van Es JH, Kuipers J, Kujala P, van den Born M, Cozijnsen M, et al. Identification of stem cells in small intestine and colon by marker gene Lgr5. Nature. 2007; 449(7165):1003–7. Epub 2007/10/16. https://doi.org/10.1038/nature06196 PMID: 17934449.